Fractal dimension from the box counting method for REV permeability estimation

CILAMCE-PANACM-2021

Tatiana Lipovetsky[1], Eduardo Guimarães Ribeiro[2], Austin Boyd[1], Luca Moriconi[3], Paulo Couto[1]

[1]*LRAP (Enhanced Oil Recovery Laboratory), Dept. of Civil Engineering, Federal University of Rio de Janeiro*
Rua Moniz Aragão Nº 360, Bloco 4 (LTEP), Cidade Universitária, 21941-594 - P.O. Box 68548, RJ, Brazil
tatianalipovetsky@petroleo.ufrj.br, austin@petroleo.ufrj.br, pcouto@petroleo.ufrj.br
[2]*Dept. of Computer Engineering and Information, Federal University of Rio de Janeiro*
Av. Athos da Silveira Ramos Nº 274, Cidade Universitária, 21941-909, RJ, Brazil
eduardo.ribeiro@nidf.ufrj.br
[3]*Dept. of Physics, Federal University of Rio de Janeiro*
Av. Athos da Silveira Ramos Nº 149, Bloco A, Cidade Universitária, 21941-909, RJ, Brazil
moriconi@if.ufrj.br

Abstract. Thomeer-based methods, widely used for permeability estimation of rock samples, rely on the determination of pore throat distributions from mercury injection capillary pressure, for both sandstones and carbonates. These methods comprise three different approaches for permeability calculation, all of them based on concepts related to the Thomeer hyperbola. In this work, for the sake of permeability evaluation, we review and adapt the expansion of the tubular bundle model of Purcell to a fractal tubular bundle for permeability calculation. Our study is motivated by the assumption that fractal theory can be used to improve upscaling procedures, since it provides the ideal mathematical tool to deal with the commonly observed self-similarity properties of complex natural media. Furthermore, fractal concepts have been introduced and presented as a well-suited approach for flow modeling because of their simple description of highly ramified spaces. Adding up to mercury injection data, the box-counting method is applied to the analysis of thin-sections of thirty limestone samples as a way to obtain their fractal dimension and hence permeability at the representative elementary volume (REV). It turns out that the fractal approach proves to be not only of straightforward application but also to improve estimates of permeability carried along the lines of Thomeer methodological principles.

Keywords: fractal dimension, permeability, tortuosity, Thomeer-Swanson.

1 Introduction

The distribution of hydrocarbons during the charging process of the reservoir is primarily controlled by the porous system. Through wettability, the porous system controls the interaction between the rock and fluids. Through the properties of porosity, permeability, relative permeability and microscopic displacement efficiency, it controls oil in place and its recovery, as shown by Clerke *et al.* [1]. Being able to predict transport properties of fluids in the porous space requires a set of statistics embodying relevant physics for statistical description. The latter ties geology and reservoir properties with important consequences for oil extraction, as per Thompson *et al.* [2]. Based on this, Thomeer [3, 4] developed a methodology for rock-typing formations through mercury injection

capillary pressure (MICP). Later, Clerke and Martin [5] incorporated the Thomeer hyperbolae [3] representing pore systems to computerized spreadsheets to fit the MICP data from the samples. The Thomeer-Swanson spreadsheet, thoroughly tested by Buiting and Clerke [6], Clerke *et al.* [1], Clerke and Martin [5], among others, has proven to be satisfactory for permeability prediction using mercury injection capillary pressure from sandstones and carbonates.

The Thomeer-Swanson spreadsheet by Clerke and Martin [4] was developed as a way of rock typing the Arab-D formation in Saudi Arabia, which was characterized thoroughly by many authors (Buiting and Clerke, [6]; Cantrell and Hagerty [7, 8]; Clerke *et al.* [1]; Swart *et al.* [9] and references therein). The spreadsheet allows to analyze the extrapolated displacement pressure P_d of MICP (Figure 1) for unimodal, bimodal and trimodal pore size distributions (PSD). The concepts behind the spreadsheet consider that the porosity group within a given PSD which contains the largest pore throats is expected to dominate the permeability, while the other groups control oil in place and irreducible water saturation.

The spreadsheet calculations return values of the permeability based either on complete PSDs or on specific pore sizes from MICP. MICP data and the corresponding bulk volume, porosity and permeability from basic petrophysics must be entered into the spreadsheet. The bulk volume capillary pressure (BV-P_c) graph should be continuous and differentiable, thereby forming at least one left-skewed pore throat histogram (LSPTH), as shown in Figure 2.

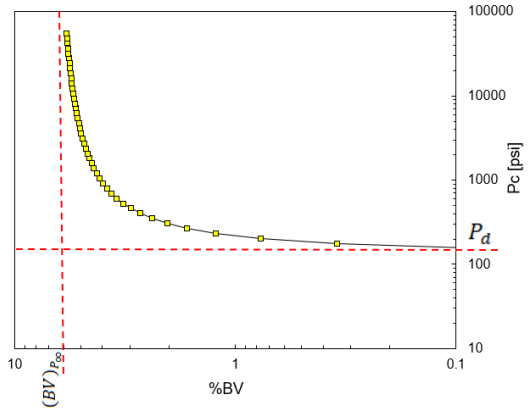

Figure 1. When plotted on log-log axes, the MICP capillary pressure P_c versus bulk volume BV curve generally resembles a hyperbola.

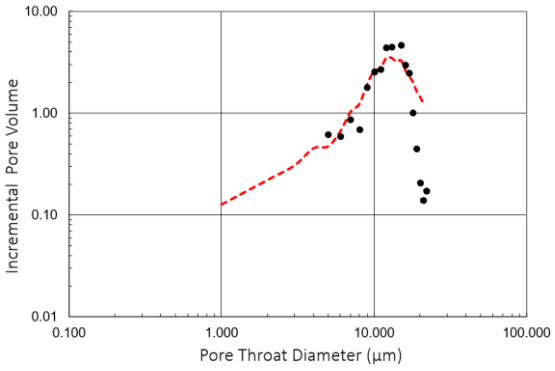

Figure 2. Thomeer's LSPTH, shown in red, derived from MICP data (black) of pressure and incremental bulk volume converted into pore throat diameters Thomeer [3], Clerke and Martin [4] and Thomeer [5].

The Thomeer-Swanson spreadsheet is based on the graphs shown in Figure 1 and Figure 2 to calculate permeability in four different manners. **The first method** is based on the Thomeer hyperbola (as seen in Figure 1) and correlates the bulk volume BV, P_d (asymptotic pressure at the limit of small values of BV) and the geometrical coefficient of the formed curve to permeability, G. The method derived an equation for the air permeability (in millidarcies) from a regression analysis of data from 165 siliciclastic and 114 carbonate samples, leading to the monomodal permeability estimation:

$$k_{air} = 3.8068\{BV/P_d\}^2 G^{-1.3334}. \tag{1}$$

The second method is the Buiting-Clerke tortuous and relative fractal tubular bundle model (B-C k integral). In this approach, Buiting and Clerke [6] expanded the tubular bundle model of Purcell for permeability [7] to a fractal tubular bundle. The model assumes that the tubes responsible for breakthrough percolation are those with the largest diameter d (radius r_d) with a tortuosity given by L/L_d, where L_d is the length of the first percolation path (or the shortest flow path associated with the largest tube of radius r_d) and L is the outer length of the sample [6]. Tortuosity can be considered as a fractal-like property, with fractal dimension D_f between 1 and 2 [13]. Here, the permeability is given as

$$k = \frac{\varepsilon^2}{4} D_f^{-2(1-D_f)Q_d} \left(\frac{L}{L_d}\right)^2 \hat{B}_v^Q(2D_f), \tag{2}$$

where D_f is the fractal dimension defining tortuosity calculated by the box counting method Amozu [8], Antoniazzi [9] and Wang *et al.*, [10] from thin-section images acquired by an electrical microscope, $\varepsilon = 2[\sigma cos\theta]_{Hg-Air} = 734dy/cm = 107psi\mu m$, P is the pressure of the injected mercury, $Q = ln(P)$ and hence $Q_d = ln\,(P_d)$. $\hat{B}_v^Q(2D_f)$ is obtained through the analysis of $\tilde{B}_v^Q(2D_f)$, which is an integral transform of the MICP fractional bulk volume (*BV)* in the *Q*-domain, as explained by Buiting and Clerke[6].

The third method is the Thomeer-based Buiting-Clerke permeability estimation (B-C k fit), where it is possible to obtain a permeability value for the single Thomeer fitted hyperbola. Considering Eq. (1) and assuming $L_d/L = 2$ and $D_f = 1.56$ (common values for carbonates), the permeability of the unimodal pore system is given by Buiting and Clerke [6]:

$$k_{BC} \approx 506\frac{BV^{\infty}}{P_d^2}e^{-4.43\sqrt{G}}. \tag{3}$$

Although the Thomeer-based methods have been widely used with a pre-fixed value of fractal dimension representing tortuosity of 1.56, there is not much evidence that calculating the fractal dimension for each sample improves the results. Thereunto, we review the box-counting methodology to calculate the fractal dimension from thin-section images of each sample using the second method (B-C k integral).

2 Methodology

2.1 Fractals

As noted by Hunt *et al.* [11], porous media have been modeled in many different ways: as random or regular sphere packs, as bundles of capillary tubes, as pore networks, and with fractal concepts. The fractal dimension represents the degree of occupation of the fractal geometry in space, indicating the irregularities of the geometrical figure.

For decades it was believed that the heterogeneities of porous media were random and uncorrelated, and would change significantly over length scales much smaller than the media's linear extent. Evidence accumulated over the years suggest, however, that natural porous media may exhibit correlations in the spatial distribution of their properties at multiple length scales. This finding can be analyzed using fractal distributions to describe how the properties of a porous medium depend on the observation scale, how the properties are correlated and how to correctly model the correlations as noted by Hunt and Sahimi [12]. Because of the self-similarity of fractals, it is possible to use fractal dimensions to aid in upscaling.

2.2 Box-Counting

Box-Counting methods involve dividing a given two-dimensional image into squares, and accounting for the squares that comprise parts of the image, as proposed by Amozu [8]. An iterative process progressively diminishes the size of the squares and sums up the parts comprising the images of interest. Through the number of squares and their lengths, it is possible to calculate the fractal dimension D_f of the image being analyzed, according to Antoniazzi [9]:

$$D_f = -\frac{log\left(\frac{N_{i+1}}{N_i}\right)}{log\left(\frac{1/L_{i+1}}{1/L_i}\right)}, \tag{4}$$

where N_i is the number of squares containing the object of interest (i.e., the pore) and L_i the integer number of divisions made on the initial side of the square, such that the maximum value for N is N_{max}, N_{max} being the total number of squares in each iteration:

$$N_{max} = L^2. \tag{5}$$

In attempts to calculate the fractal dimension, a computational box-counting code was built in C++ to obtain the fractal dimension from thin section images (2D) obtained with a microscope. In a first iteration, the thin section is not divided but remains as it is. The second iteration is done by dividing the sides of the initial square into two

segments ($L = 2$). Images for the first, second and third iterations for a 2-D case are shown in Figure 3.

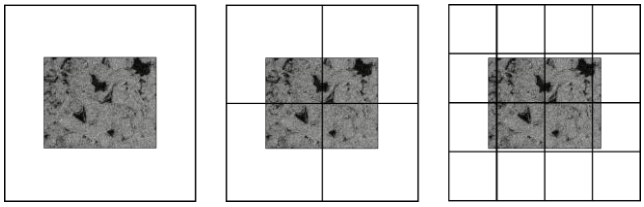

Figure 3. Schematics showing the process of dividing images, starting from the first iteration, and proceeding to the second and third iterations.

The code reads the images and differentiates pores from solid material and the background through color differentiation. Hence, N keeps track when a square or box intercepts a pore, as shown in Figure 4. In this figure, pores are represented in black, therefore the squares accounted for N are shown on the right in solid lines in black, while the shaded grey define squares that are not accounted for N. Iterations are done until the square reaches a predetermined side length, in pixels, according to the image resolution.

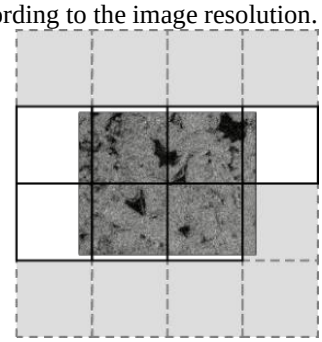

Figure 4. A representative zoom showing a division in squares after the n^{th} iteration (here, n=3).

For images with different side lengths, such as a rectangle of 10 x 20 units, the first square in the first iteration can be extrapolated such that the short side becomes as large as the largest one (e.g., a 20 x 20 units square extrapolated from a 10 x 20 unit rectangle) without affecting N and L.

Another problem the box-counting code can deal with is related to odd image lengths, such as an 11 x 11 units image (e.g., centimeters) square, as shown in Figure 5. The first iteration then faces no problem since no division is made. But from the second iteration on it is necessary to add units of squares. Assume having a side of 11 units, then the second iteration would account for 2 segments of 5.5 units, a non-integer. If 5-unit segments are chosen, a 1-unit segment is left behind the calculation (shaded in grey), which requires another 5-unit segment to be added. In this case, the number of squares goes from 4 squares with 5.5 units each, to 9 squares with 5 units each. L is then hence the rounded-up division of the integer part of the first trial segment (i.e., L = round-up of 11/5 = 3).

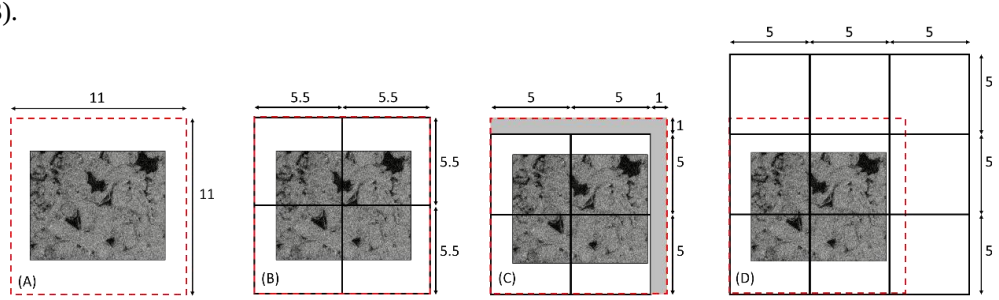

Figure 5. Box counting iterations for divisions that do not return an integer length: (A) the first iteration (in red); (B) second iteration returning a non-integer length; (C)Adoption of the closest smallest integer for the segment;

(D) newly added squares of the same length as in step C.

Finally, it is possible to calculate the fractal dimension of the pore system via box counting. By using linear regression, the fractal dimension is obtained by plotting log (N) versus $log\ (1/L)$ of all iterations on a cartesian plot. The absolute value of the slope of the fitted line is the fractal dimension. The fractal dimension obtained from thin-sections, which reflects the tortuosity, is used to calculate the REV permeability.

2.3 Thin sections

Quantitative data regarding porosity and the pore size distribution can be obtained from direct or indirect petrophysical investigations. Direct investigations are commonly performed using gas or mercury injections, while the indirect studies are performed using thin sections. Thin section petrographical analyses require careful examination, and are usually bi-dimensionally limited.

High-resolution thin section images are obtained from petrographic microscopes that scan thin polished sections or cover slips of rocks. Blue color epoxy dye is typically used to expose pores, thus distinguishing them from the crystal structure of the rock as pointed by Buono *et al.* [14]. Basic petrophysical porosity and permeability data also provide a reference for thin sections, which sometimes produce lower micro- and macro-porosities because of the relatively small area covered by the images as discussed by Carneiro *et al.* [15].

After scanning a rock, the acquired image is segmented to account for pore and porosity using the red-green-blue (RGB) spectrum. A binary image is then generated, where pores are represented in black, and solids in white. For this, the ImageJ software, developed by Schneider *et al.* [16], was used. This process is shown in Figure 6. Posteriorly to generating a binary image, pixels are counted and the porosity and pore size distribution are computed. The fractal dimension is also calculated based on the box-counting method.

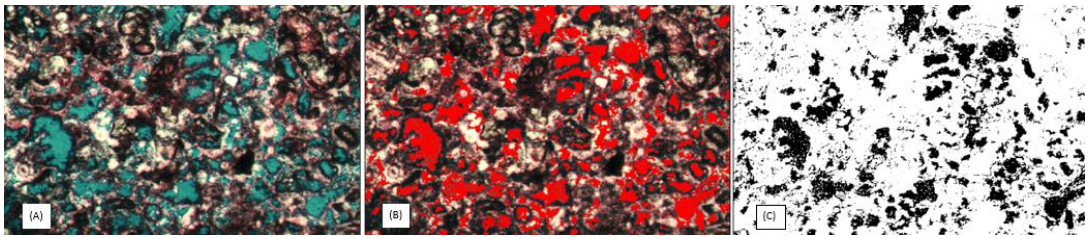

Figure 6. Illustration of ImageJ processing: (A) Limestone blue-stained thin section, showing pores in blue; (B) segmentation, showing pores in red; (C) binary image, showing pores in black (Courtesy of World Wide Rock Catalog, by CoreLab).

2.4 MICP

Mercury capillary pressure analyses can be used to determine pore geometry and to predict the behavior of immiscible fluid pairs in the porous medium as described by Churcher *et al.* [17]. The Washburn equation, given by Eq. (6), provides a simple relationship to convert mercury pressure into a pore size and is a special case of the Young-Laplace equation, as explained by Gregg and Sing [18]:

$$P_c = (\rho_w - \rho_{nw}) g_a h = \frac{2\sigma cos\theta_c}{r_{cap}}, \tag{6}$$

where P_c is the capillary pressure (e.g., in kPa), σ is the surface tension between air and mercury (480 mN/m), θ is the contact angle (equal to 140^o for air-mercury) and r_{cap} is the pore throat radius (μm). g_a is the acceleration due to gravity, h is the height above the free surface, σ is interfacial tension and r_{cap} is the capillary tube radius.

3 Results and discussion

The results presented in this work cover the analyses performed on 30 limestone samples retrieved from a quarry in North-East Brazil (one sample) and 29 oil wells worldwide, similar to those found in the Pre-salt

reservoirs. Results from the routine basic petrophysical measurements are used as the standard porosity and permeability values. The objective was to calculate the representative elementary volume (REV) permeability of the studied carbonate samples, the majority of which showed bimodal pore size distributions, using the Thomeer-Swanson spreadsheet. The individual values of fractal dimension D_f were calculated for each sample using the box-counting method for each thin-section and resulting permeability values were compared to the standard calculations of the spreadsheet (fixed D_f).

First, MICP pore throat size distribution was obtained for all samples and entered in the Thomeer-Swanson spreadsheet. Initially, the methods were used for calculating permeability without modifications in the calculations. Subsequently, **Method 2** (B-C k integral) had its standard D_f value modified for each sample to the D_f found from the thin-section analysis. The tortuosity definition of L/L_d was kept equal to 0.5 in all calculations.

The accuracy of measured versus fitted or calculated data are reflected by several statistical measures, such as R-squared (R^2), and the root mean square error (RMSE). Several measurements involved logarithmic scale data for which the root mean square log-transformed error (RMSLE) are calculated. The RMSLE parameter comparing the accuracy of the calculated permeability calculated (k_{cal}) versus the measured permeability from basic petrophysics (k_{meas}) is given by Eq. 7, where N_s represents the amount of data:

$$RMSLE = \sqrt{\frac{1}{N_s}\sum_{i=1}^{N_s}[logk_{cal} - logk_{meas}]^2}\,. \tag{7}$$

Figure 7 compares the measured permeability to the permeability estimations from the Thomeer-based models, where dashed lines indicate a variation equal to ± 20% of the permeability. Comparison of the RMSLE values summarized in Table 1 indicate that the Buiting-Clerke tortuous and relative fractal tubular bundle model (B-C k integral) with fractal dimension calculated individually for each sample (Eq. 2) is the most accurate method, while the remaining presented methods are the least accurate ones amongst those studied here. The least accurate method for the studied samples is the monomodal Thomeer hyperbola method (Eq. 1).

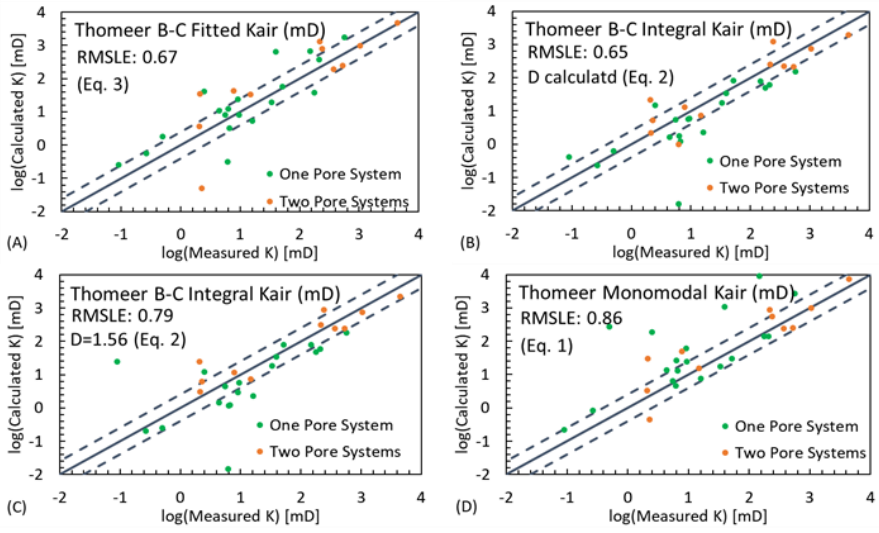

Figure 7. RMSLE values for (A) Thomeer-based Buiting-Clerke permeability estimation (B-C k fit); the Buiting-Clerke tortuous and relative fractal tubular bundle model (B-C k integral) with fractal dimension calculated individually for each sample (in B) and with the suggested global value of 1.56 for the fractal dimension (in C); and (D) the monomodal Thomeer hyperbola method.

Table 1. RMSLE values for the Thomeer-based methods.

Method	Monomodal (Method 1)	B-C Integral (Method 2)	B-C Integral fixed D_f (Method 2)	B-C Fitted (Method 3)
RMSLE	0.86	0.65	0.79	0.67

4 Conclusions

The Thomer-Swanson spreadsheet was partially implemented with the intention of showing that calculating the fractal dimension, a property of the tortuosity present in porous media, can be beneficial for permeability estimations using the Thomeer-based approaches. Comparison of the calculated permeability to the measured permeability indicates that Buiting-Clerke tortuous and relative fractal tubular bundle model (B-C k integral, **Method 2**) with fractal dimension calculated individually for each sample using the box-counting technique applied to thin-sections estimates permeability more accurately than the other approaches presented.

Acknowledgements. This research was carried out in association with the ongoing R&D project ANP nº 20163-2, "Análise Experimental da Recuperação de Petróleo para os Carbonatos do Pré-sal do Brasil através de Injeção Alternada de CO2 e Água" (UFRJ/Shell Brasil/ANP), sponsored by Shell Brasil under the ANP R&D levy as "Compromisso de Investimentos com Pesquisa e Desenvolvimento". This study was financed in part also by CAPES (Coordenação de Aperfeiçoamento de Pessoal de Nível Superior, Brazil) and CNPq (National Council for Scientific and Technological Development, Brazil.

Authorship statement. The authors hereby confirm that they are the sole liable persons responsible for the authorship of this work, and that all material that has been herein included as part of the present paper is either the property (and authorship) of the authors, or has the permission of the owners to be included here.

References

[1] E. A. Clerke *et a.*, "Application of Thomeer Hyperbolas to decode the pore systems, facies and reservoir properties of the Upper Jurassic Arab D Limestone, Ghawar field, Saudi Arabia: A 'Rosetta Stone' approach," *GeoArabia*, vol. 13, no. 4, pp. 113–160, 2008.

[2] A. H. Thompson, A. J. Katz, and C. E. Krohn, "The microgeometry and transport properties of sedimentary rock," *Adv. Phys.*, vol. 36, no. 5, pp. 625–694, Jan. 1987.

[3] J. H. M. Thomeer, "Introduction of a Pore Geometrical Factor Defined by the Capillary Pressure Curve," *J. Pet. Technol.*, vol. 12, no. 03, pp. 73–77, 1960.

[4] E. A. Clerke and P. R. Martin, "Thomeer Swanson excel spreadsheet and FAQ's and user comments." SPWLA 2004 Carbonate Workshop, Noordwijk, 2004.

[5] J. H. Thomeer, "Air Permeability Aas a Function of Three Pore-Network Parameters.," *JPT, J. Pet. Technol.*, vol. 35, no. 4, pp. 809–814, 1983.

[6] J. J. M. Buiting and E. A. Clerke, "Permeability from porosimetry measurements: Derivation for a tortuous and fractal tubular bundle," *J. Pet. Sci. Eng.*, vol. 108, pp. 267–278, 2013.

[7] W. R. Purcell, "Capillary Pressures - Their Measurement Using Mercury and the Calculation of Permeability Therefrom," *J. Pet. Technol.*, vol. 1, no. 02, pp. 39–48, Feb. 1949.

[8] A. Amosu, H. Mahmood, P. Ofoche, and M. Imsalem, "Interactive Estimation of the Fractal Properties of Carbonate Rocks," pp. 1–11, 2018.

[9] R. L. Antoniazzi, "Aplicação do método box counting para a estimativa da dimensão fractal de figuras planas digitalizadas," Universidade Federal de Santa Maria, 2007.

[10] H. Wang, Y. Liu, Y. Song, Y. Zhao, and J. Zhao, "Fractal dimension analysis on pore structure of artificial cores using magnetic resonance imaging," *2012 2nd Int. Conf. Consum. Electron. Commun. Networks, CECNet 2012 - Proc.*, pp. 2593–2596, 2012.

[11] A. Hunt, R. Ewing, and B. Ghanbarian, *Percolation Theory for Flow in Porous Media*, Lecture No., vol. 880. Cham: Springer International Publishing, 2014.

[12] A. G. Hunt and M. Sahimi, "Flow, Transport, and Reaction in Porous Media: Percolation Scaling, Critical-Path Analysis, and Effective Medium Approximation," *Rev. Geophys.*, vol. 55, no. 4, pp. 993–1078, 2017.

[13] B. Mandelbrot, "How Long Is the Coast of Britain? Statistical Self-Similarity and Fractional Dimension," *Science (80-.).*, vol. 156, no. 3775, pp. 636–638, May 1967.

[14] A. Buono *et a.*, "Quantitative digital petrography: Full thin section quantification of pore space and grains," *SPE Middle East Oil Gas Show Conf. MEOS, Proc.*, vol. 2019-March, 2019.

[15] G. Carneiro *et a.*, "Evaluating pore space connectivity by NMR diffusive coupling," *SPWLA 55th Annu. Logging Symp. 2014*, 2014.

[16] C. A. Schneider, W. S. Rasband, and K. W. Eliceiri, "NIH Image to ImageJ: 25 years of image analysis.," *Nat. Methods*, vol. 9, no. 7, pp. 671–5, Jul. 2012.

[17] P. L. Churcher, P. R. French, J. C. Shaw, and L. L. Schramm, "Rock Properties of Berea Sandstone, Baker Dolomite, and Indiana Limestone," in *SPE International Symposium on Oilfield Chemistry*, 1991.

[18] S. Gregg and K. Sing, "Adsorption. Surface area and porosity.," *Acad. Press. London.*, 1982.